CrossMark

ORIGINAL ARTICLE

Morphology, pore size distribution, and nutrient characteristics in biochars under different pyrolysis temperatures and atmospheres

Zhongxin Tan[1] · Junhua Zou[1] · Limei Zhang[1] · Qiaoyun Huang[1]

Abstract To evaluate the agronomic potential of biochar, we prepared a series of biochars using rice straw waste under the limited oxygen cracking condition (CO_2 or N_2) and the different pyrolysis temperatures including 300, 400, 600, and 800 °C. The results showed that morphology structure, specific surface area, pore size distribution, and element contents of the biochars were superior to the biochars prepared under traditional inert atmosphere (N_2) and the same four pyrolysis temperatures. In comparison with the rice straw, pore structure of biochars was mainly mesoporous and more developed, average pore size decreased, and BET-specific surface area increased with the increase of temperature from 300 to 800 °C. Biochars distributed abundant mesopores and macropores under 400 and 600 °C; the maximum macropores of the biochar were shaped under 600 °C. Concentration of phosphorus (P) and potassium (K) increased significantly with increasing temperature, while that of nitrogen (N) first increased and then decreased and reached a maximum at 400 °C. In addition, taking these physiochemical properties into consideration, we drew a conclusion that the optimum quality biochar could acquire under the work conditions of 400 °C and CO_2 atmosphere, which was supposed to provide theoretical guidance for biochar returning to soil.

Keywords CO_2 atmosphere · Biochars · Nutrient content · Pore structure

✉ Zhongxin Tan
   tanzx1977@163.com

[1] College of Resources and Environment, Huazhong
   Agricultural University, Wuhan 430070,
   People's Republic of China

Introduction

Biochar is the solid product of biomass pyrolysis when the feedstocks are heated under complete or partial exclusion of oxygen [1–3]. Various common residual forms of the biomass, including wood, rice husk, straw, bamboo, and animal wastes, can be utilized as a feedstock of biochar for the pyrolysis process [4]. In recent years, biochar has received considerable interest in recent years due to its potential roles in carbon sequestration and soil amendment [5–7]. Biochar characteristics change widely according to preparation conditions (e.g., temperature, atmosphere, raw material, pyrolysis rate, residence time, etc.) [8, 9]; therefore, a wide diversity of its composition and property is expected [10, 11]. Biochar derived from wood has higher carbon (C) amount than those obtained from herbaceous feedstocks [12, 13], but they are depleted in nitrogen (N) [14], Conversely, livestock manures are more enriched in nitrogen, phosphorus, and micronutrients, and as a consequence, their pyrolysis produces biochars with higher nutrient content [15]. Extensive analyses contribute to a better understanding of thermochemical transformations that take place during pyrolysis, providing support to the consumers on the use of a specific biochar for each particular agro-ecosystem. Table 1 summarizes the studies about the effects of preparation conditions on the physicochemical properties of biochar in recent years.

Seen from Table 1, scholars have studied mostly about the effects of feedstocks and pyrolysis temperatures on the physicochemical properties of biochars, and the preparation atmosphere they choose mostly are N_2 atmosphere or anoxybiotic conditions. CO_2, one of the weak oxidation gases, has been widely used as the gasification agent for the synthesis gas and the activator for the preparation of activating CO_2, while it is not widely used in the biochar preparation process as the pyrolysis atmosphere (especially

Table 1 Evolution of biochar characteristics/functions along different preparation conditions (temperatures, feedstocks, and atmospheres)

Characteristics	Temperatures: low → high	References
Carbon categories	Transition char → amorphous char → composite char → turbostratic char (pine wood shavings and tall fescue grass, 100–700 °C, oxygen-limited conditions)	[8]
Electrical conductivity	Increased first and then decreased and reached its peak at 400 °C (sewage sludge, 300–700 °C, N_2 atmosphere)	[25]
Formation mechanism	Dehydration → condensation/aromatization (honey mesquite, 200–650 °C, oxygen-limited conditions)	[40]
Field capacity	Increased first and then decreased (corn stover, magnolia leaves, and apple wood, 300–700 °C, oxygen-limited conditions, high field capacity, and low hydrophobicity at pyrolysis temperatures between 400 and 600 °C)	[41]
Specific surface area	Increased constantly (Douglas fir wood, Douglas fir bark, and poplar wood, 350–600 °C, N_2 atmosphere)	[42]
	Increased first and then decreased and reached its peak at 600 °C (pine wood, green waste, wheat straw, and spray-dried algae, 300, 450, 600, and 750 °C, N_2 atmosphere)	[43]
Organic carbon content	Decreased constantly (pine wood, 300–700 °C, oxygen-limited conditions)	[44]
Transport	Decreased constantly (wheat straw and pine needle, 350 and 550 °C, anaerobic conditions)	[45]
Water-soluble intermediates	Increased to a maximum and then decreased (amorphous and crystalline cellulose, 100–350 °C, Ar atmosphere, get a maximum at 250 and 270 °C, respectively)	[46]
Nitrogen content	Increased to a maximum and then decreased (pine wood, 100–700 °C, oxygen-limited conditions, achieved a maximum at 400 °C)	[8]
Inorganic composition	Silicon: amorphous to crystalline (rice straw, 150–700 °C, oxygen-limited conditions)	[47]
	Phosphorus: phytate → orthophosphate/pyrophosphate (plant and manure, 350, 500, 650 and 800 °C, N_2 atmosphere)	[48]
	Calcium: whewellite → calcite (*Eucalyptus saligna* wood, 400 °C and 550 °C)	[49]
	Potassium leaching rate increased (wheat straw, poplar wood, and spruce wood, 400, 460 and 525 °C, oxygen-limited conditions)	[50]
	Sulfur: inorganic sulfur decreased, organosulfur increased (oak and corn stover, 500, 600, and 850 °C, N_2 atmosphere)	[51]

using straw as the feedstocks), considered as a good carrier gas in biochar preparation for its simple storage, safety, nontoxicity, and extensive sources. Rice straw is selected as a feedstock for preparing biochar due to its abundance in China, it is worth noting that the preparation atmospheres are N_2 or oxygen-limited conditions, and there have been scarce studies reporting about the characteristics of rice straw biochar prepared under CO_2 atmosphere. At present, many uncertainties exist in defining "biochar quality." For example, biochar used for carbon sequestration purposes would be evaluated based on its decomposition rates and its effect on the native soil organic matter pool, whereas biochar used as an adsorbent would be evaluated on its pore structure and high specific surface area [16–20]. However, biochar value for the purpose of returning has always been the focus in scenic areas. The highly aromatic structure of biochar and its specific surface characteristics along with its high porosity have been considered as the main reason for altering the soil structure (density, pore size distribution, and aggregate stability), influencing the water dynamics, affecting soil pore size distribution, and water holding capacity [21]. Pore characteristics are a major contributor to the properties of biochar; it can be considered as the

high-quality biochar through soil improvement (promotion of soil porosity and fertility) after applying biochar to soil. Given this, this article chooses rice straw as the feedstock to prepare a series of biochars at a range of 300–800 °C under CO_2 atmosphere, at the same time, the other four rice straw biochars were prepared under the inert atmosphere (N_2) and the same four pyrolysis temperatures, separately, and focuses on the characteristics of the products through biochar yield calculation, FESEM–EDS, BET-specific surface, and other analysis methods to figure out the preparation condition of high-quality biochar, which is expected to provide a theoretical reference for the preparation condition of biochar and its reasonable use in agriculture.

Materials and methods

Materials

Rice straw is known as the agricultural biomass waste, obtained from the experimental field of Huazhong Agricultural University, Wuhan, China. At first, the rice straw containing more than 15 wt% of moisture was dried naturally

Table 2 Yields of biochars prepared under different conditions

Pyrolysis temperature (°C)	Yields in CO_2 atmosphere (%)	Yields in N_2 atmosphere (%)
300	54.67	56.26
400	40.35	40.42
600	33.17	33.49
800	28.38	29.13

and cut into rice straw chips (10–20 mm long); the sample size of 20 g per batch experiment was used for the biochar preparation, marked B0, and set aside. Then, a part of the rice straws was crushed and sieved to obtain a sample of particle size less than 1 mm for subsequent analysis.

Biochar preparation

The pyrolysis of rice straw chips (10–20 mm long) was carried out in a fluidized bed pyrolysis furnace. For each trial, about 20 g of sample was loaded into the sample carrier. The biochars were produced using a stepwise procedure, which was heated up gradually to the target temperature of 300, 400, 600, and 800 °C, and the heating rate was 20 °C/min) with CO_2 (99.99%, 40 L/h) purging to provide a reductive atmosphere in the pyrolysis process, and remained at the target temperatures for about 20 min. The resultant biochar sample was allowed to cool to ambient environment, and then was weighed and recorded as the solid charcoal yield, as shown in Table 2. The biochars were labeled as BC300, BC400, BC600, and BC800 accordingly. BC represented biochars prepared under CO_2 atmosphere, while the suffix number represents the carbonization temperature. The preparation steps of biochars prepared under N_2 atmosphere mostly were the same as the biochars preparation; CO_2 would be replaced by N_2 (99.999%) at a flow of 40 L/h to provide a reductive atmosphere in the furnace, and then, the biochar products were marked BN300, BN400, BN600, and BN800, separately. BN represented biochars prepared under N_2 atmosphere, and 300, 400, 600, and 800 represented the pyrolysis temperature, as well. All the biochars were stored in a desiccator. They were then homogeneously subsampled for analyses. Straw and the biochars prepared under different conditions can be shown in Fig. 1. Element analysis of rice straw and biochar was done as shown in Table 3.

Fig. 1 Straw and the biochars prepared under different conditions

Table 3 Elemental analysis of rice straw and biochars

Samples	C (wt%)	H (wt%)	O (wt%)	N (wt%)	P (wt%)	K (wt%)
B0	36.8	5.51	53.65	1.3	0.27	2.47
BC300	44.35	3.99	45.56	1.65	0.41	4.04
BC400	46.64	2.49	43.03	1.48	0.55	5.81
BC600	47.03	1.05	43.67	1.13	0.62	6.50
BC800	44.82	0.52	46.15	0.94	0.66	6.91
BN300	45.73	4.08	44.64	1.68	0.36	3.50
BN400	48.05	2.71	41.92	1.42	0.52	5.38
BN600	47.80	1.24	42.83	1.04	0.62	6.47
BN800	45.19	0.57	46.24	0.85	0.62	6.53

Samples (rice straw, biochars) characterization

A number of methods were used to investigate the physicochemical characteristics (e.g., morphology, nutrient contents, specific surface area, and pore size distribution) of the biochars. All analyses were conducted in duplicate. Morphology and nutrient contents: Field emission scanning electron microscopy (FESEM) with energy dispersive spectrometer (EDS) was used to determine the morphology and nutrient contents of virgin biomass and char particles. The samples for cross-sectional images were prepared by placing them into epoxy resins and were polished with platinum to ensure electrical conductivity of the surface and were then observed under the same magnifications by FESEM. The EDS line spectra were acquired by drawing arrows at 1000× magnification for 300 s to achieve a sufficient signal-to-noise ratio. The results were autocorrected and optimized by Inca software.

BET-specific surface area and pore size distribution: specific surface area and pore size distribution of the biochar were determined using a BET-N_2; according to BET multiplayer adsorption theory, the isothermal adsorption of N_2 at 77 K was studied using an automatic adsorption equipment (Micromeritics, ASAP 2020, USA) to analyze the pore structure characteristics of the samples. Before the adsorption measurements, the sample was degassed at 150 °C under a vacuum for 6 h. The total pore volume was calculated at a relative pressure of 0.99. The BET surface area (S_{BET}), average pore size, and total volume (V) of the samples were determined by application of the Brunauer–Emmett–Teller (BET) equation, t plot method, and single point adsorption total pore volume analysis, respectively. The pore size distribution was analyzed by the density-function theory (DFT) method, which can be used to calculate the distribution of micro-, meso-, and macropores, simultaneously.

Results and discussion

Effect of pyrolysis temperature and atmosphere on the physical characteristics of biochar

Effect of pyrolysis temperature and atmosphere on biochar morphology characteristics

Temperature   FESEM was employed to observe the surface physical morphology of the samples. Surface morphology evaluation of the biochars produced at different pyrolysis temperatures under N_2 atmosphere can be compared from the FESEM micrographs (Fig. 2). It can be seen that the structure of the parent material (rice straw) was disordered consisted of solid cells strongly bonded, and slits derived from the interior of the straw and no micropores were observed, and just several mesopores and macropores existed, which generated for the mass transmission during the growth process as a plant, giving an irregular and rough appearance instead of the pore structure. Morphology of the biochars varied with the different temperatures; with increase in pyrolysis temperature, the fissures and slits in biochar surface were found to be more prominent. The external surface of BN300 displayed several irregular pore structures of different sizes, and the pore shape was not complete; parts of the straw structures still maintained in BN300, indicating incomplete pyrolysis at 300 °C. When the pyrolysis
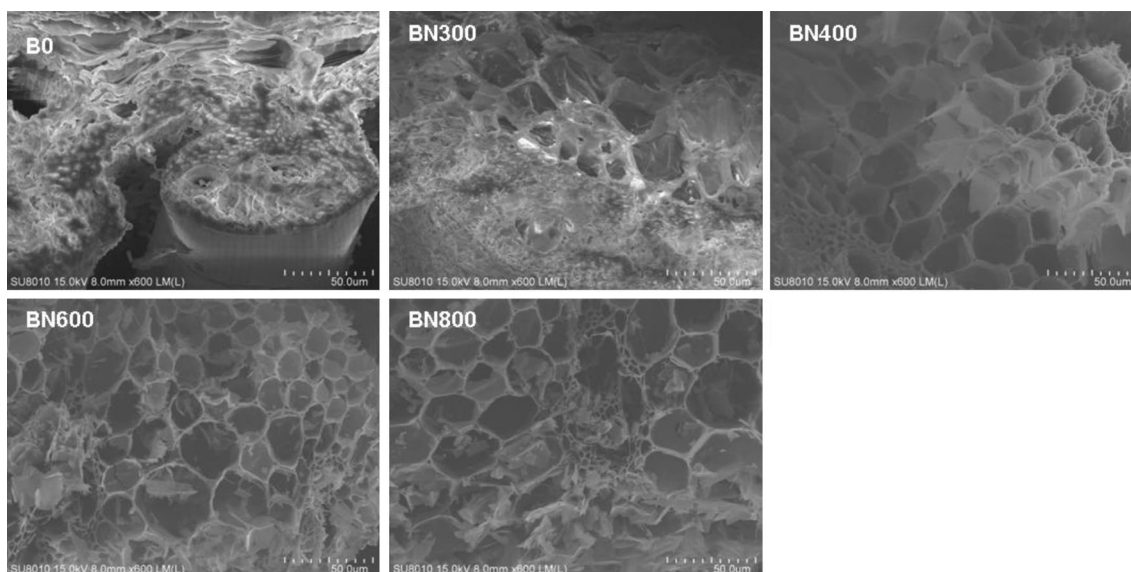

Fig. 2 Cross-sectional FESEM images of the rice straw and biochars prepared under different pyrolysis temperatures (N_2)

temperature rose to 400 °C, the pore structure exhibited in order, increasing pores, compact pore structure, developed porosity, and shaped integrity in BN400. With the temperature rising from 400 to 600 °C, the pores in the marrow of biochar enlarged and started to crack outward, leading the appearance of larger pores, a certain amount of micropores generated and developed close to the macropores. At temperatures higher than 600 °C, micropores developed further, the collapse of pore structure was more obvious, marrows fell in the way of clusters, but most of the structure was still reserved. The results showed the pyrolysis process facilitated the pore structure; however, some macropores with large pore size would collapse at high temperatures in accompany with biochar micropore development.

Atmosphere Figure 3 shows the effects of different pyrolysis atmospheres on the morphology of the rice straw biochars. The main char structure of the biochar was more and more obvious and rich with increasing temperature, similar to the morphology change of municipal sewage sludge biochar produced at 400–600 °C [22]. Pituello et al. [23] observed the similar changes and thought that the interactions among components of the biomass might affect pyrolysis behavior of the various constituents and increase the heterogeneity of biochars. However, biochars prepared under the two atmospheres differed in the morphology characteristics. At temperatures higher than 300 °C, micropores of the biochars (N_2) formed mostly in the adjacent marrow of macropores, while the micropores would generated densely in somewhere of the biochars (CO_2) other than appeared in the adjacent marrow of macropores. At the temperature of 300 °C, it can be seen parts of primary rice straw tissues in BN300 instead of BC300, indicating that CO_2 improved the pyrolysis process and presented more pores in BC300, that was to say, pore structure in BC300 was more developed than BN300. In both atmospheres at 400 °C, the process

Fig. 3 Cross-sectional FESEM images of the biochars prepared under different pyrolysis atmospheres
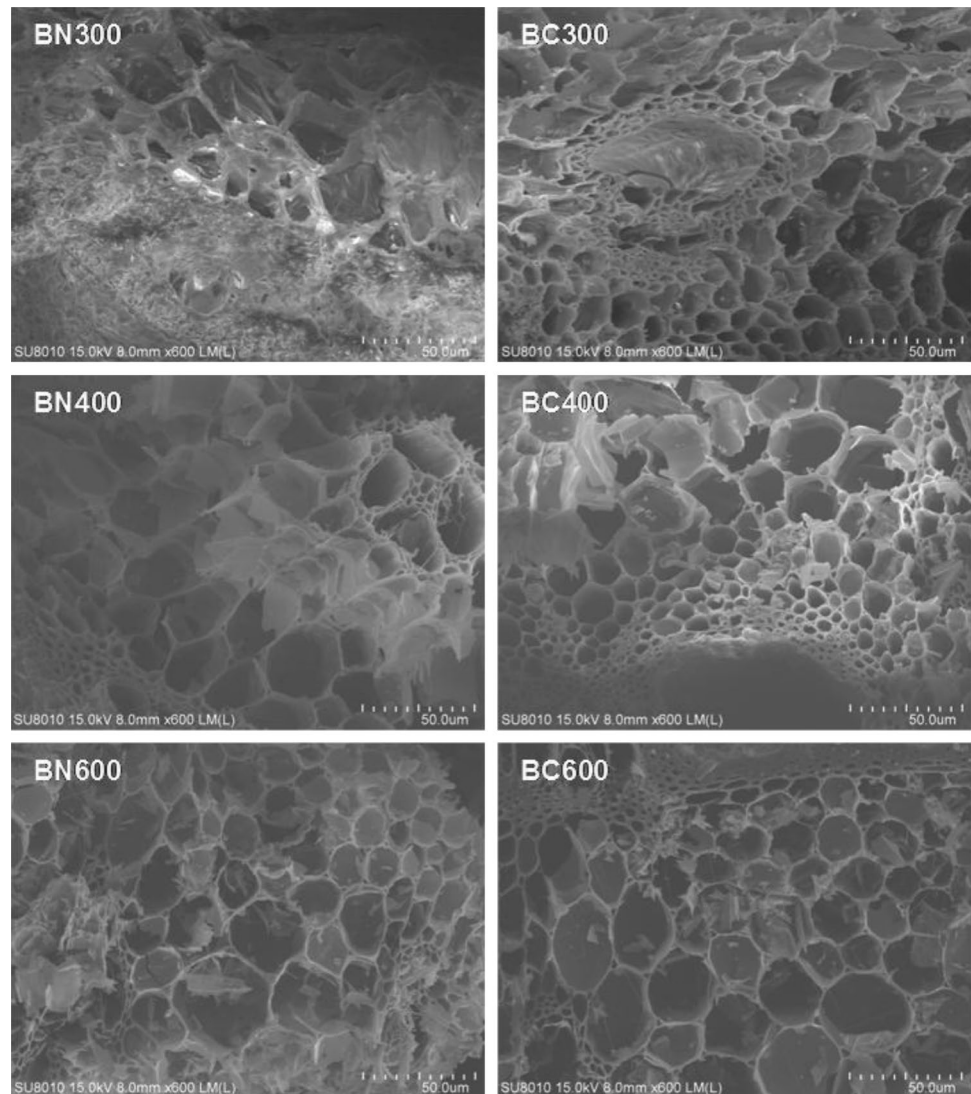
of volatile release produced a highly porous char structure in BC400 and BN400, but it was much thicker of the pore walls in BC400 compared with BN400, which deserves higher mechanical strength relative to BN400, and the char structure of BC400 would not be destroyed instantly when incorporated into soil, pore sizes varied from micropores to macropores in BC400, while seen simple pore sizes distribution in BN400 (macropores and micropores close to the macropores), showing that CO_2 atmosphere affected the formation of pores. At temperatures higher than 400 °C, char structure in BC600 started to collapse; however, BN600 depicted slight collapse, leading a poorer mechanical strength as well. All the morphology structures presented a certain difference in the biochars under the two atmospheres. Morphology of BC showed more developed and firmer char structures, higher mechanical strength, and more extensive forms of the pore sizes. Lee et al. [24] reported similar results that micro- and mesopores were highly developed in biochar prepared under CO_2 instead of N_2 at the temperature of 650 °C. We concluded that the quality of biochars obtained under CO_2 atmosphere was superior to that of N_2 atmosphere.

Effects of pyrolysis temperature and atmosphere on the specific surface area of samples (rice straw, biochars)

Temperature　Biochar pores were divided into micropores (<2 nm), mesopores (2–50 nm), and macropores (>50 nm), according to pore size [25]. As shown in Table 4, pore structure of rice straw and biochar products was mainly mesoporous; for the biochars, the average pore size decreased, but the BET-specific surface area increased with an increase of pyrolysis temperature. Due to the devolatilization characteristics of rice straw in heating process, specific surface area and pore volume of the rice straw sample were as small as 1.167 m²/g and 0.00479 cm³/g, and they increased gradually from 1.809 m²/g and 0.00670 cm³/g to 24.435 m²/g and 0.0211 cm³/g, respectively, with the rise of the pyrolysis temperature from 300 to 800 °C, which was similar to the previous observations for the biochars pro-

duced from cotton stalk [26], reed [27], and rice straw [28–30]. Compared with raw rice straw, the release of the mass as volatile matter only enlarged the surface area of chars at 300 °C, to a small extent, and the surface area only increased to 1.809 m²/g, which may be due to the degradation of the hemicellulose, and thus caused the formation of a few pores for the release of volatile matter and discharge of gaseous product, leading the slight increase of the surface area. Continuous increase in the temperature up to 400 °C and the surface area of BN400 increased to 4.649 m²/g, showing an improvement by a large margin for some micropores appearance. Several researchers suggested that the degradation of cellulose was occurring during 250–450 °C [31–33], and the appearance of micropores showed that the cellulose may be decomposed. However, with the temperature increasing further to 800 °C, a continuous increase of the surface area, causing the total surface area to increase from 4.649 to 24.435 m²/g. This increase may be attributed to the increasing micropores for the decomposition of hemicellulose, cellulose, and lignin at high temperatures. From the comparison of these dates, it can be concluded that higher temperatures were favourable to the preparation of biochars with high specific surface area. And FESEM image presented evidence that the surface area of biochar increased with pyrolysis temperature, as well; however, similar observations by Li et al. [34] reported that pyrolysis at the higher temperature causes a larger specific surface area in biochars.

Atmosphere　Table 5 gave the comparisons of the surface structure features of the biochars produced from different pyrolysis atmospheres. It was observed that the biochars prepared under two different atmospheres had different surface structure features, though they had similar variation trend with increasing temperature. The specific surface areas of BC were higher than BN at the same temperature; at temperatures lower than 600 °C, the effects of the two atmospheres on biochar-specific surface area were not as obvious as that at temperatures higher than 600 °C. Under

Table 4 Comparisons of the surface structure features between rice straw and biochars at different temperatures

Samples	S_{BET} (m²/g)	Total pore volume (cm³/g)	Average pore size (nm)	Pore volume of micropore (cm³/g)
B0	1.167	0.00479	16.407	0.000432
BN300	1.809	0.00670	14.807	0.000711
BN400	4.649	0.0142	12.242	0.00184
BN600	10.273	0.0148	5.613	0.00426
BN800	24.435	0.0211	3.455	0.00959

Table 5 Comparisons of the surface structure features between biochars at different atmospheres

Samples	S_{BET} (m²/g)	Total pore volume (cm³/g)	Average pore size (nm)	Pore volume of micropore (cm³/g)
BC300	2.105	0.00957	18.178	0.000832
BC400	4.985	0.0146	11.684	0.00196
BC600	13.511	0.0158	4.673	0.00535
BC800	303.731	0.161	2.114	0.122
BN300	1.809	0.00670	14.807	0.000711
BN400	4.649	0.0142	12.242	0.00184
BN600	10.273	0.0148	5.613	0.00426
BN800	24.435	0.0211	3.4551	0.00959

CO_2 atmosphere, when the pyrolysis temperature rose from 600 to 800 °C, the specific surface area had a significant increase form 13.511 to 303.731 m^2/g, while under N_2 atmosphere, the specific surface area just increased form 10.273 to 24.435 m^2/g, showing an increase in small scale compared with the former, which may be due to the different properties of the two atmospheres. N_2, an inert gas, had limited effects on the char structure. Unlike N_2, CO_2 can serve as an activator, CO_2 activation will become more vigorous once at a higher temperature, the presence of CO_2 was benefit for improvement of the micropores, and specific surface area of BC800 surpassed BN800 markedly.

Effects of pyrolysis time, temperature, and atmosphere on pore size distribution of biochars

Time Residence time affects biochar properties. For example, the average pore size of biochar is shown in Fig. 4. The average pore size of biochar increases with increasing residence time from 10 to 30 min at 600 °C and in the N_2 atmosphere. When the residence time is 20 min, the average pore size of biochar reaches 0.1232 μm, corresponding to an 8.45% higher pore size compared to 10 min. Increasing the residence time from 20 to 30 min is associated with a decrease in the average pore size. The pore size decreases 3.57% between 20 and 30 min. The pore structure of biochar is closely connected to its average pore size, and the pore structure is a primary factor affecting its adsorption ability. Therefore, the pore structure of biochar can be adjusted by controlling the residence time, because there is a critical time for biomass material carbonization.

Temperature Pore size distributions of the rice straw sample and biochars represented by BN were showed in Fig. 5. There were almost no micropores in the rice straw, showing rare mesopores and macropores, indicating that the structure of rice straw was extremely underdeveloped. In all the biochars, the number of micropores, mesopores, and macropores was enhanced after heating the rice straw
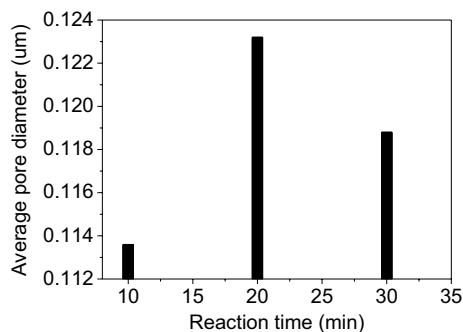

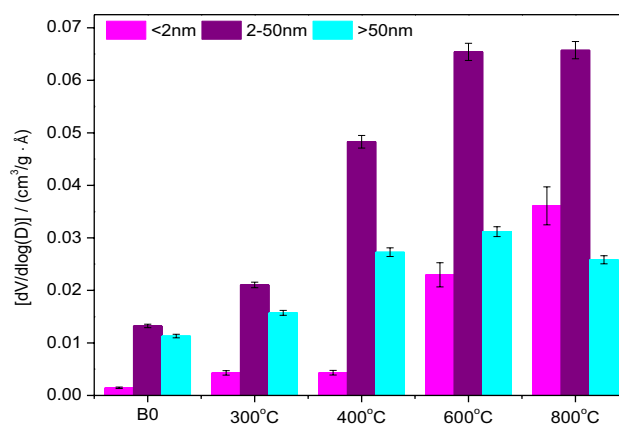**Fig. 4** Effect of residence time on the average pore size of biochar

Fig. 5 Changes of the pore size distribution in rice straw sample and biochars prepared at different temperatures (N_2)

at different temperatures. Contrast to the rice straw, the pore structures of all the biochars were relative developed with different degree. Micropores was generally low for biochars produced at all temperatures, especially in low temperatures (300, 400 °C), which were slightly higher than that of rice straw, number of micropores only changed a little, when the pyrolysis temperature rose from 300 to 400 °C, micropores in BN300 were nearly equal to that in BN400. It showed a continuous increase of micropores with the pyrolysis temperature increasing from 400 to 800 °C, and a significant improvement of micropores occured between 300 and 400 °C, which were consistent with FESEM- and BET-specific surface analysis. Mesopores were the dominant pores in all the biochars, which increased greatly with an increase in temperature from 300 to 600 °C; then, with further increase in temperature, the increasing extent of mesopores was lowered, reaching its maximum value at 800 °C. In comparison with micropores and mesopores, macropores has the variation that increased first and then decreased with increasing temperature and reached its peak at 600 °C. The number of macropores had the order of BN600 > BN400 > BN800 > BN300 > rice straw, which achieved the largest growth at temperature ranged from 300 to 400 °C, indicating that it was not conducive to the formation of macropores at the temperature which was too high or too low. Therefore, biochar produced at high temperature was beneficial to the generation of micropores, while mesopores and macropores had extensive pore size distribution at moderate temperature. Hence, the pore structure of the biochar was relatively developed at 400 °C.

Atmosphere To describe the effects of atmospheres on the pore characteristics during pyrolysis, a pore size distribution profile was obtained based on the DFT, as shown in Fig. 6. All the biochars had the pore size distributions which varied from 1.7 to 300 nm, CO_2 pyrolysis generated biochars
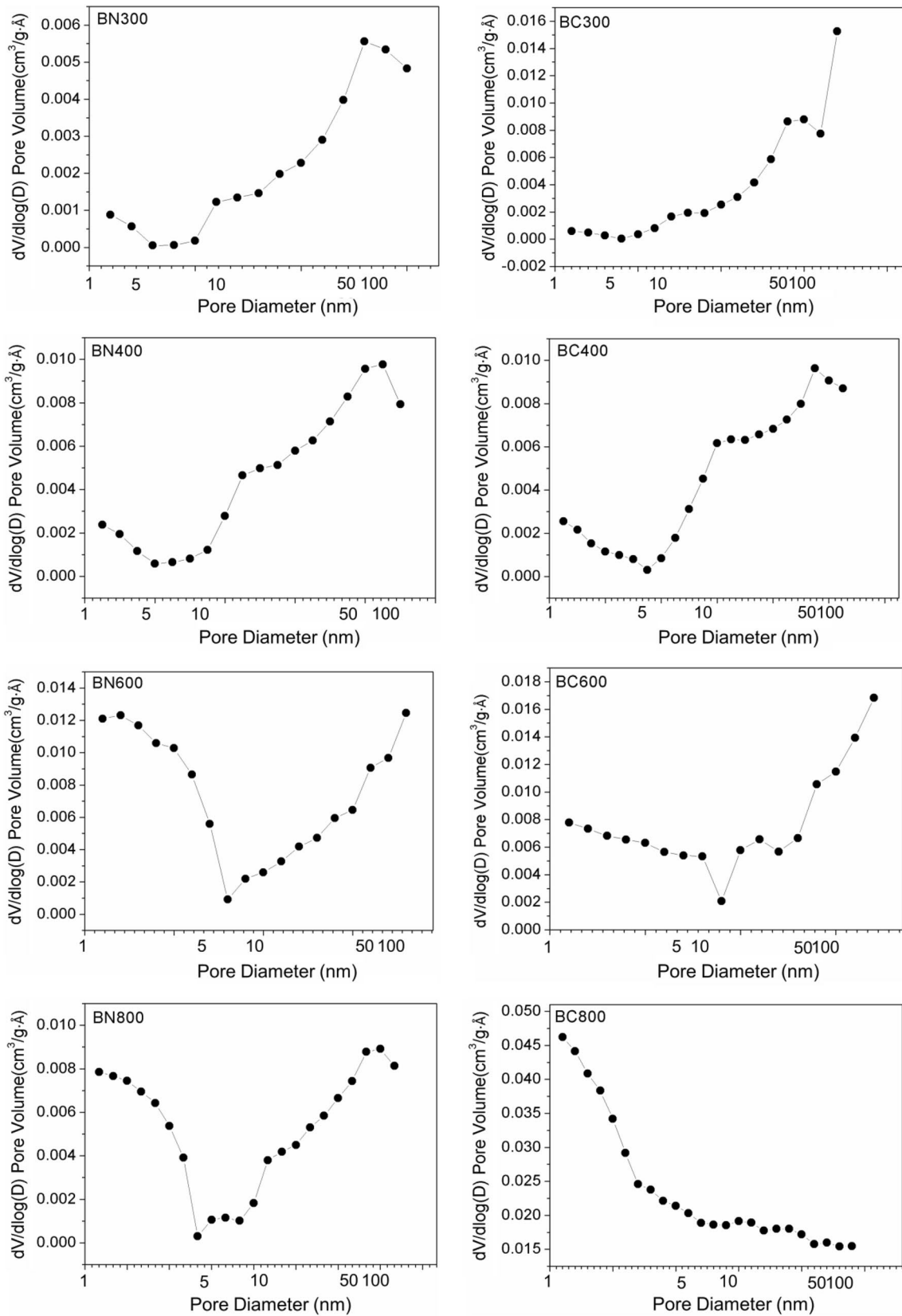
Fig. 6 Effects of the pyrolysis atmosphere on the pore size distribution of the biochars

with higher micropores, mesopores, and macropores as observed from Fig. 6. It can be concluded that the porosity in the range of micropores, mesopores, and macropores was better developed under CO_2 atmosphere. Pore size distribution began to present a certain differences even at low temperatures in BC and BN, especially for the mesopores. Pore size distribution of BC was relatively sparse at pore diameters above 15 nm and the majority of macropores found between 75 and 300 nm; among the four biochars (BC300, BC400, BC600, and BC800), BC600 had the largest member of macropores. While pore size distribution of BN was relatively sparse at pore diameters 5–15 nm, macropores focused mostly between the pores of sizes 75 and 275 nm, which showed more extensive mesopores and macropores distribution in CO_2 pyrolysis generated biochars. On increasing the temperature, there was an increasing disparity (in the quantities) between the macropores in BC and BN, which was the same as mesopores–mesopores and micropores–micropores. It can be seen that the numbers of pores (micropores, mesopores, and macropores) in BC800 were significantly higher than the numbers of corresponding pores in BN800. The pore size distribution had a significant increase of micropores in BC800, and in the range of mesopores (2–15 nm), more intensive pores size distribution of BC800 contrast with BC800, which was attributed to the fact that CO_2 could serve as an important activator and react with the char structure of biochars at high temperatures, showing a promotion of the pore structure, especially the

micropores. BC800 has the largest numbers of mesopores and macropores, while the numbers of micropores were up to the maximum in BC600.

Effects of pyrolysis temperature and atmosphere on the nutrients in biochars

Pyrolysis temperature effects on variation of nutrients (N, P, and K) in biochars (N_2)

EDS technique was applied to detect the variation of nutrients (N, P, and K) in rice straw and biochars produced at various temperatures and in N_2 atmosphere (shown in Fig. 7a–c) and the RR (retention rate shown in Fig. 7d), which was between 0 and 100%. The lower RR indicated fewer elements remained in biochars. It was known that the rice straw and biochars were rich in K, and followed by N nutrient, while P content was relatively low. All the three kinds of nutrient elements showed regular changes with the rise of pyrolysis temperature.

Total N content in biochar significantly increased initially in low-temperature biochars (300 and 400 °C), and then significantly decreased for high-temperature biochars (600 and 800 °C), getting a maximum and minimum at 400 and 800 °C, respectively. This may be due to the loss rate of N which was less than the mass loss rate of rice straw at the temperature below 400 °C, leading to the enrichment of nitrogen in low-temperature biochars (300 and 400 °C).

Fig. 7 **a–c** Changes in total N, P, and K concentration in rice straw sample and biochars at various temperatures, respectively, **d** RR for the nutrient contents of rice straw sample and biochars at various temperatures
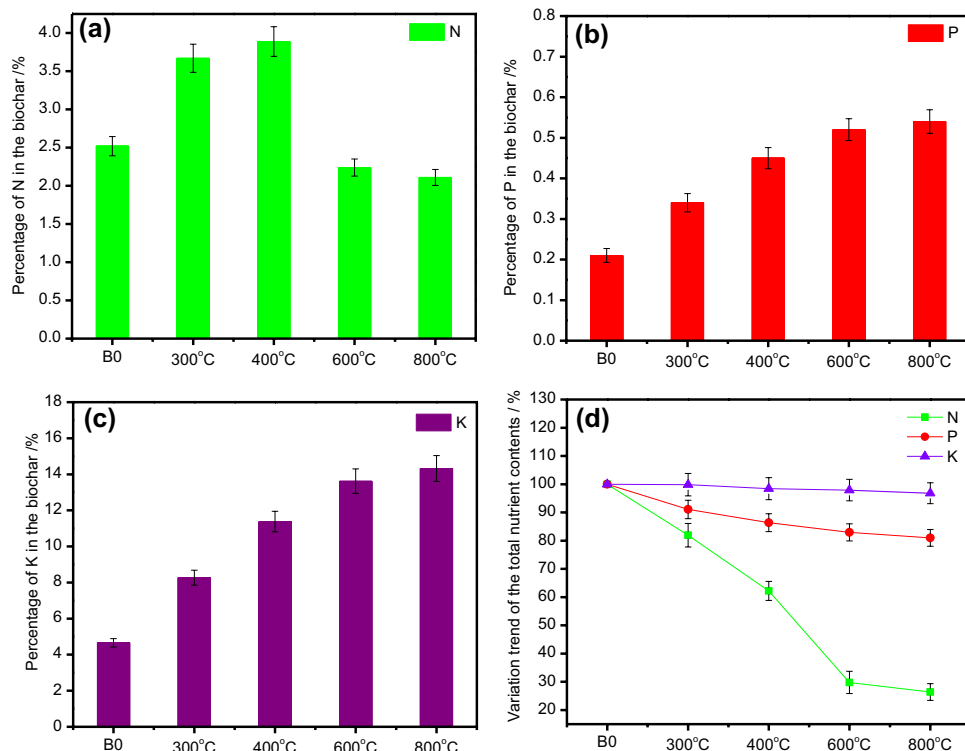
However, with the temperature increasing further, the volatilisation of N became more vigorous; a decrease of total N in the biochar was observed in high-temperature biochars (600 and 800 °C). Total N content of 400 °C biochar increased from the feedstock concentrations by 54.37%; for the 800 °C biochar compared to feedstock, total N content decreases by 16.27%. As for the retention rate of N (NRR), with the pyrolysis temperature increasing from 300 to 800 °C, NRR decreased constantly from 81.92 to 26.38%; a sharp decrease was observed during 400–600 °C. The previous research has shown that N was removed through loss of the NH_4–N and NO_3–N fraction as well as the loss of volatile matter containing N groups [35]. Our study indicated that relatively high proportion of nitrogen would be conserved at low pyrolysis temperatures, and high-temperature pyrolysis would present a massive loss of N.

Total content of P in the rice straw sample was 0.21%. Total content of P in biochars increased from 0.34 to 0.54% with the pyrolysis temperature increasing from 300 to 800 °C, indicating that P was associated with the inorganic fraction of the rice straw, showing a similar trend in sludge pyrolysis biochar reported by Mustafa [36]. The maximum P was 0.54% in BN800 at 800 °C, which increased 157% compared to the rice straw. The RR of P indicated 81.00–91.07% of P was retained in biochars, which might be attributed to the fact that P contained in rice straw was associated with thermo-stable phosphate minerals that was difficult to decompose and became more crystallized with increasing temperature [37].

Total content of K in the rice straw sample was 4.66%. With the pyrolysis temperature increasing from 300 to 700 °C, the content of K in the biochars increased from 8.27 to 14.32%. This result indicated that the enrichment of K in biochars was intensified remarkably with the rise of pyrolysis temperature, which has the similar trend as compared to P. And the RR of K indicated that 96.8–99.83% of K was retained in biochars. The concentration of K in biochars increased with increasing pyrolysis temperatures and this increment may be due to its high vaporization temperature.

Pyrolysis atmosphere (CO_2 and N_2) effects on variation of nutrients (N, P, and K) in biochars

The EDS spectra of the biochars prepared under CO_2 and N_2 atmospheres revealed their elements variation (Fig. 8). It showed that a relatively C content in biochars prepared under CO_2 atmosphere decreased by 6.58–17.15%; C content in biochars prepared under the two atmospheres had a same variation trend with increasing temperature (increased first and then decreased and reached its peak at 400 °C), while O content of BC surpassed BN, which was attributed to the pyrolysis and gasification reaction of biochars prepared at CO_2 atmosphere, the element of O can

be introduced into the biochar through a series of oxidation reactions during the gasification process. The higher nutrient contents (N, P, and K) and according RRs were observed in BC suggested better nutrient characteristics. N content in BC increased by 3.57–8.17% compared with N_2 atmosphere. Ren indicated that the formation of H free radicals of biochars can make CO_2 inhibit the production of gases (HCN, HNCO, etc.) through the pyrolysis process [38]. There were almost no volatilization of P and K in the rice straw pyrolysis process, which differed from N. P and K would be intensified with the rise of pyrolysis temperature; however, biochar yields (Table 2) were lower BC than BN, hence causing the high content of P and K in BC.

Optimum preparation approach of the biochar for its returning use

Nutrients were easy to lose during the pyrolysis of rice straw; biochars also varied in morphology features and pore structure with the preparation conditions. Through the analysis we have characterized above, the theoretical mechanism of the high-quality biochar for the purpose of returning was obtained, as shown in Fig. 9. Rice straw heated in a relatively low temperature (300 and 400 °C) would get larger retention rate of the nutrients (N, P, and K) in biochars. It was porous structure of the biochar morphology that pyrolyzing at temperatures above 300 °C (400, 600, and 800 °C). Extensive pore size distributions were observed at temperatures higher than 300 °C (400, 600, and 800 °C), all the pores of the rice straw biochars were mesopores, macropores were only second to only mesopores other than the biochar prepared at 800 °C, and with the temperature increasing further to 800 °C, micropores would increase significantly. The effects of these pores on soil quality are different. Specifically, macropores might improve soil aeration and water infiltration; mesopores could adsorb macromolecules which cannot enter the microporous structure, and provided the carrier for the preservation of soil fertility, micropores might adsorb and retain nutrients to improve soil fertility. However, studies have shown that the larger macropores and mesopores can play a relatively obvious role in soil amendment compared to the micropores [25, 39]. Then, combining with economic energy consumption, it was suggested that 400 °C was the optimum temperature for the preparation of biochars. In comparison with the two atmospheres (N_2, CO_2), we found that characteristics (morphology, pore size distribution, and nutrients content) of BC were superior to BN at the same pyrolysis temperature, and hence, CO_2 atmosphere was more appropriate than N_2 atmosphere to produce biochars. Therefore, the optimum preparation approach of the biochar for its returning use should be in 400 °C and CO_2 atmosphere.
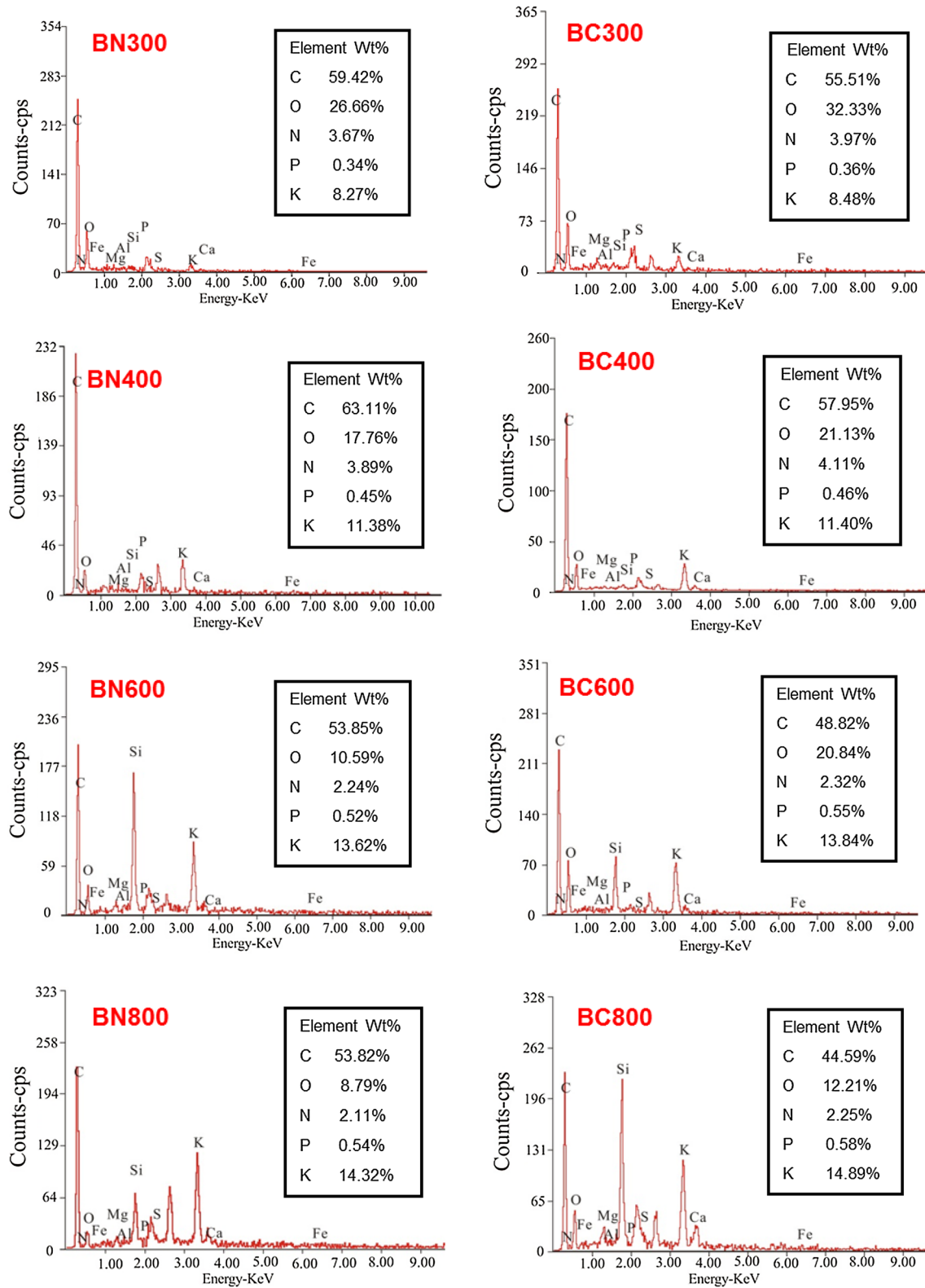
Fig. 8 EDS spectra quantification of the biochars (BN300, BN400, BN600, BN800, BC300, BC400, BC600, and BC800), respectively
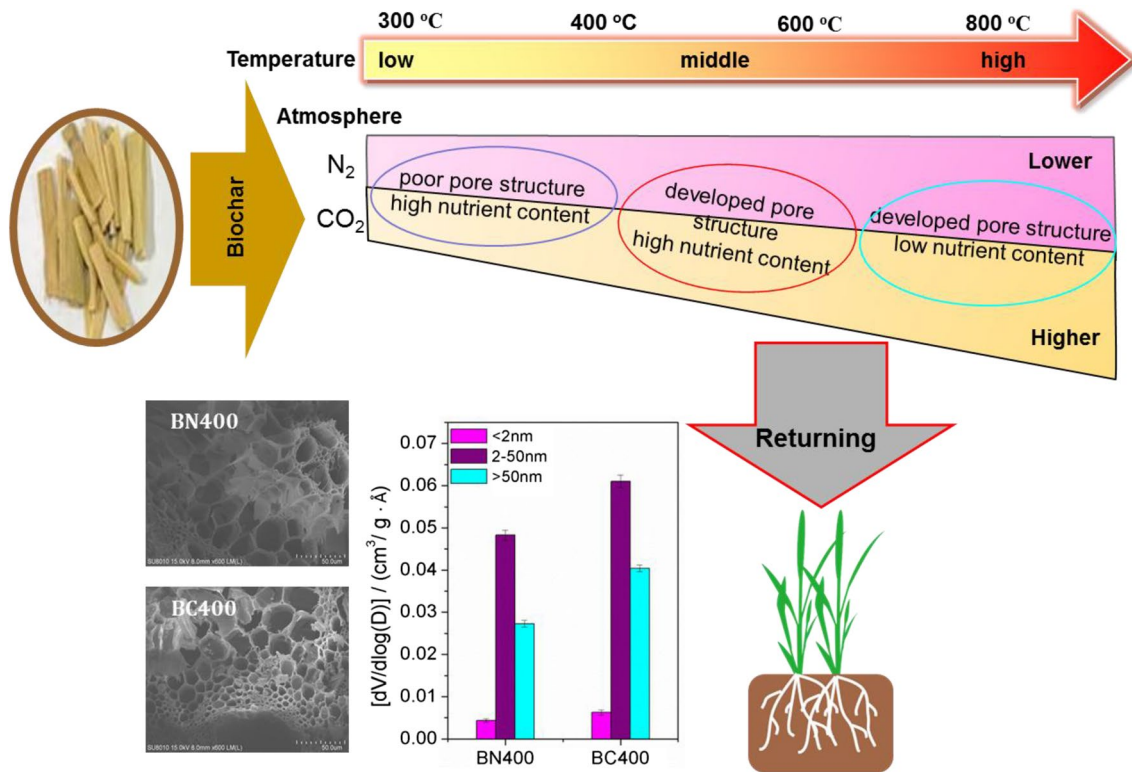
Fig. 9 Effect of residence time on the average pore size of biochar at 600 °C and in the N_2 atmosphere [52]

Conclusions

The results of FESEM showed that both the pyrolysis temperature and atmosphere have effects on biochar morphology, the raw rice straw could not be pyrolyzed completely at 300 °C, char structure gradually developed, more developed pore structure in biochars prepared at intermediate temperate (400 °C), and a collapse was seen in high temperatures (600 and 800 °C). CO_2 prepared biochars had more developed pore structure, thicker wall, and higher mechanical strength which was not easy to destroy after their incorporation into soil. Total pore volume and specific surface area increased with increasing temperature, CO_2 prepared biochars exhibited a high total pore volume and specific surface area than N_2 prepared biochars. The rice straw-derived biochars were rich in K, and followed by N nutrient, while P content was relatively low. With the rise of pyrolysis temperature, the content of N in the biochars increased first and then decreased and reached its peak at 400 °C, while the content of P and K always increased; all the three nutrients' content showed relatively lower content in N_2 prepared biochars than that of CO_2. The result from BET analysis indicated that extensive pore size distribution in biochars pyrolyzes at temperatures above 300 °C. There were significant increases of macropores and mesopores at intermediate temperatures (400 and 600 °C), and porosity in the range of micropores, mesopores, and macropores was better developed under CO_2 atmosphere. 400 °C and CO_2 atmosphere were considered as the optimum operating conditions of high-quality rice straw-derived biochars for returning.

References

1. Wardle DA, Nilsson MC, Zackrisson O (2008) Fire-derived charcoal causes loss of forest humus. Science 320(5876):629
2. Xu G, Lü YC, Sun JN, Shao HB, Wei LL (2012) Recent advances in biochar applications in agricultural soils: Benefits and environmental implications. Clean Soil Air Water 40(10):1093–1098
3. Sohi S (2013) Biomass, bioenergy and the sustainability of soils and climate: what role for biochar? In: EGU general assembly conference. EGU general assembly conference abstracts
4. Deng X (2012) Effects of Giant reed biochar on nitrogen bio-availability in the agricultural soil. Ocean University of China, Qingdao **(in Chinese)**
5. Yue Y, Cui L, Lin Q, Li G, Zhao X (2017) Efficiency of sewage sludge biochar in improving urban soil properties and promoting grass growth. Chemosphere 173:551–556
6. Brassard P, Godbout S, Raghavan V (2016) Soil biochar amendment as a climate change mitigation tool: key parameters and mechanisms involved. J Environ Manag 181:484–497

7. Biederman LA, Harpole WS (2013) Biochar and its effects on plant productivity and nutrient cycling: a meta-analysis. Glob Change Biology Bioenergy 5:202–214

8. Keiluweit M, Nico PS, Johnson MG, Kleber M (2010) Dynamic molecular structure of plant biomass-derived black carbon (biochar). Environ Sci Technol 44(4):1247–1253

9. Cha JS, Park SH, Jung S, Ryu C, Jeon J, Shin M et al (2016) Production and utilization of biochar: a review. J Ind Eng Chem 40:1–15

10. Gaskin JW, Steiner C, Harris K, Das KC, Bibens B (2008) Effect of low-temperature pyrolysis conditions on biochar for agricultural use. Trans ASABE 51:2061–2069

11. Ro KS, Cantrell KB, Hunt PG (2010) High-temperature pyrolysis of blended animal manures for producing renewable energy and value-added biochar. Ind Eng Chem Res 49:10125–10131

12. Zabaniotou A, Stavropoulos G, Skoulou V (2008) Activated carbon from olive kernels in a two-stage process: industrial improvement. Biores Technol 99:320–326

13. Jeffery S, Bezemer TM, Cornelissen G, Kuyper TW, Lehmann J, Mommer L et al (2013) The way forward in biochar research: targeting trade-offs between the potential wins. Glob Change Biol Bioenergy 7:11–13

14. Cao XD, Harris W (2010) Properties of dairy-manure-derived biochar pertinent to its potential use in remediation. Biores Technol 101:5222–5228

15. Cantrell KB, Hunt PG, Uchimiya M, Novak JM, Ro KS (2012) Impact of pyrolysis temperature and manure source on physicochemical characteristics of biochar. Biores Technol 107:419–428

16. Park SH, Cho HJ, Ryu C, Park Y (2016) Removal of copper(II) in aqueous solution using pyrolytic biochars derived from red macroalga *Porphyra tenera*. J Ind Eng Chem 36:314–319

17. Sun Y, Zhang JP, Guo F, Zhang L (2016) Hydrochar preparation from black liquor by CO_2 assisted hydrothermal treatment: optimization of its performance for Pb^{2+} removal. Korean J Chem Eng 33:2703–2710

18. Ahmadi M, Kouhgardi E, Ramavandi B (2016) Physico-chemical study of dew melon peel biochar for chromium attenuation from simulated and actual wastewaters. Korean J Chem Eng 33:2589–2601

19. Li G, Zhu W, Zhu L, Chai X (2016) Effect of pyrolytic temperature on the adsorptive removal of p-benzoquinone, tetracycline, and polyvinyl alcohol by the biochars from sugarcane bagasse. Korean J Chem Eng 33:2215–2221

20. Ruthiraan M, Mubarak NM, Thines RK, Abdullah EC, Sahu JN, Jayakumar NS et al (2015) Comparative kinetic study of functionalized carbon nanotubes and magnetic biochar for removal of Cd^{2+} ions from wastewater. Korean J Chem Eng 32:446–457

21. Verheijen F, Jeffery S, Bastos AC, van der Velde M, Diafas I (2010) Biochar application to soils. A critical scientific review of effects on soil properties, processes and functions. European Commission Joint Research Centre, Institute for Environment and Sustainability, Luxemburg, p 149

22. Jin J, Li Y, Zhang J, Wu S, Cao Y, Peng L et al (2016) Influence of pyrolysis temperature on properties and environmental safety of heavy metals in biochars derived from municipal sewage sludge. J Hazard Mater 320:417

23. Pituello C, Francioso O, Simonetti G, Pisi A, Torreggiani A, Berti A et al (2015) Characterization of chemical–physical, structural and morphological properties of biochars from biowastes produced at different temperatures. J Soils Sediments 15:792–804

24. Lee J, Yang X, Cho S, Kim J, Lee SS, Tsang DCW et al (2017) Pyrolysis process of agricultural waste using CO_2 for waste management, energy recovery, and biochar fabrication. Appl Energy 185:214–222

25. Yuan H, Lu T, Huang HY, Zhao DD, Kobayashi N, Chen Y (2015) Influence of pyrolysis temperature on physical and

26. Chen Y, Yang H, Wang X, Zhang S, Chen H (2012) Biomass-based pyrolytic polygeneration system on cotton stalk pyrolysis: influence of temperature. Bioresour Technol 107:411

27. Peng P, Lang Y, Wang X (2016) Adsorption behavior and mechanism of pentachlorophenol on reed biochars: pH effect, pyrolysis temperature, hydrochloric acid treatment and isotherms. Ecol Eng 90:225–233

28. Lu K, Yang X, Shen J, Robinson B, Huang H, Liu D et al (2014) Effect of bamboo and rice straw biochars on the bioavailability of Cd, Cu, Pb and Zn to Sedum plumbizincicola. Agric Ecosyst Environ 191:124–132

29. Zhang R, Li Z, Liu X, Wang B, Zhou G, Huang X et al (2017) Immobilization and bioavailability of heavy metals in greenhouse soils amended with rice straw-derived biochar. Ecol Eng 98:183–188

30. Jian MF, Gao KF, Yu HP (2016) Effect of different pyrolysis temperatures on the preparation and characteristics of bio-char from rice straw. Acta Sci Circumst 36:1757–1765 **(in Chinese)**

31. Shen DK, Gu S (2009) The mechanism for thermal decomposition of cellulose and its main products. Biores Technol 100(24):6496–6504

32. Vamvuka D, Sfakiotakis S (2011) Effects of heating rate and water leaching of perennial energy crops on pyrolysis characteristics and kinetics. Renew Energy 36(9):2433–2439

33. Yang HP, Yan R, Chen HP, Zheng CG, Lee DH, Liang DT (2006) In-depth investigation of biomass pyrolysis based on three major components: hemicellulose, cellulose and lignin. Energy Fuels 20(1):388–393

34. Li L, Lu YC, Liu YY, Sun HW, Liang ZY (2012) Adsorption mechanisms of cadmium(II) on biochars derived from corn straw. J Agro-Environ Sci 31(11):2277–2283 **(in Chinese)**

35. Bagreev A, Bandosz TJ, Locke DC (2001) Pore structure and surface chemistry of adsorbents obtained by pyrolysis of sewage sludge-derived fertilizer. Carbon 39(13):1971–1979

36. Mustafa KH, Vladimir S, Chan KY, Ziolkowski A, Nelson PF (2011) Influence of pyrolysis temperature on production and nutrient properties of wastewater sludge biochar. J Environ Manag 92(1):223–228

37. Zheng H, Wang ZY, Deng X, Zhao J, Luo Y, Novak J et al (2013) Characteristics and nutrient values of biochars produced from giant reed at different temperatures. Biores Technol 130:463–471

38. Ren QQ, Zhao CS, Wu X, Liang C, Chen XP, Shen JZ et al (2010) Formation of NO_x precursors during wheat straw pyrolysis and gasification with O_2 and CO_2. Fuel 89(5):1064–1069

39. Lehmann J, Joseph S (2009) Biochar for environmental management: science and technology. Earthscan 25(1):15801–15811

40. Harvey OR, Herbert BE, Kuo LJ, Louchouarn P (2012) Generalized two-dimensional perturbation correlation infrared spectroscopy reveals mechanisms for the development of surface charge and recalcitrance in plant-derived biochars. Environ Sci Technol 46:10641–10650

41. Kinney TJ, Masiello CA, Dugan B, Hockaday WC, Dean MR, Zygourakis K et al (2012) Hydrologic properties of biochars produced at different temperatures. Biomass Bioenergy 41(5):34–43

42. Suliman W, Harsh JB, Abu-Lail NI, Fortuna AM, Dallmeyer I, Garcia-Perez M (2016) Influence of feedstock source and pyrolysis temperature on biochar bulk and surface properties. Biomass Bioenergy 84:37–48

43. Ronsse F, Hecke SV, Dickinson D, Prins W (2013) Production and characterization of slow pyrolysis biochar: influence of feedstock type and pyrolysis conditions. Glob Change Biol Bioenergy 5(2):104–115

chemical properties of biochar made from sewage sludge. J Anal Appl Pyrol 112:284–289

44. Zhou ZL, Shi DJ, Qiu YP, Sheng D (2010) Sorptive domains of pine chars as probed by benzene and nitrobenzene. Environ Pollut 158(1):201–206

45. Wang DJ, Zhang W, Hao XZ, Zhou DM (2013) Transport of biochar particles in saturated granular media: effects of pyrolysis temperature and particle size. Environ Sci Technol 47(2):821–828

46. Liu DW, Yu Y, Wu HW (2013) Differences in water-soluble intermediates from slow pyrolysis of amorphous and crystalline cellulose. Energy Fuels 27(3):1371–1380

47. Xiao X, Chen B, Zhu L (2014) Transformation, morphology, and dissolution of silicon and carbon in rice straw-derived biochars under different pyrolytic temperatures. Environ Sci Technol 48(6):3411–3419

48. Uchimiya M, Hiradate S (2014) Pyrolysis temperature-dependent changes in dissolved phosphorus speciation of plant and manure biochars. J Agric Food Chem 62(8):1802–1809

49. Singh B, Singh BP, Cowie AL (2010) Characterisation and evaluation of biochars for their application as soil amendment. Aust J Soil Res 48(7):516–525

50. Kloss S, Zehetner F, Dellantonio A (2012) Characterization of slow pyrolysis biochars: effects of feedstocks and pyrolysis temperature on biochar properties. J Environ Qual 41(4):990–1000

51. Cheah S, Malone SC, Feik CJ (2014) Speciation of sulfur in biochar produced from pyrolysis and gasification of oak and corn stover. Environ Sci Technol 48(15):8474–8480

52. Lin XF, Zhang J, Yin YS (2009) Study on fractal characteristics of biomass chars. Biomass Chem Eng 43:10–12